The Characteristics of an Electroless Nickel/ Immersion Gold Plated PWB Surface Finish and the Quality of BGA Solder Joints

Grazyna Koziol, Aneta Arazna and Wojciech Steplewski*
Tele and Radio Research Institute
Ratuszowa, Poland

New formulations of electroless nickel/immersion gold (ENIG) processes which minimize the possibility of the black pad phenomenon, meet the requirements of today`s complex PWBs and can withstand the rigors of multiple assembly techniques including wire bonding, connector and key contacts, as well as EMI shielding. However, as the usage of these processes has increased, a problem has been occasionally found on occasional ball grid array (BGA) pads. A fractured solder joint sometimes appears after assembly or mechanical shocking. The interfacial fracture problem appears to occur more frequently on finer pitched parts with smaller pads, than on larger pads. The defective solder joints could be readily pulled apart, revealing a darkened nickel surface (black nickel phenomenon). This problem is unpredictable and often noted during product use. In this paper, investigations of thickness, solderability and corrosion resistance of electroless nickel/ immersion gold coatings on PWBs from two producers are presented. The reflow soldering process of BGA components with SAC solder paste including flux: type ROL0 or ROL1, were done on these boards. The BGA solder joints were examined optically, using x-ray inspection and after microsectioning. Elemental data was obtained by scanning electron microscopy with energy dispersive spectroscopy.

Keywords: *Electroless nickel, immersion gold, ENIG, corrosion, anodic polarization, solderability, interfacial cracking*

Introduction

Electroless nickel/immersion gold (ENIG) has been relied on as a durable, corrosion-resistant surface finish in the electronics packaging industry. It can withstand the rigors of multiple reflows, allowing for complex lead-free package assembly.[1] A new generation of ENIG processes has been developed toward solving the "black nickel" problem.[2-4]

However, as the usage of this process increased, a problem was first found on BGA (ball grid array) components. An open and fractured solder joint sometimes became apparent on some pads of the PWB after assembly. When such a solder joint fell victim to the black pad effect, the removed component revealed a darkened pad with evident non-wetting. The problem described as a "BGA black pad problem" or an "interfacial fracture of BGA packages" appears more frequently on finer pitched components with smaller pads, than on larger pads.[5] As surface mount technology (SMT) migrates towards smaller package dimensions, awareness of this problem has increased.

Many studies to understand the causes of black pads have been undertaken. Generally it is believed that the problem was caused by excessive or uncontrolled phosphorus co-deposition during electroless nickel plating.

More recent investigations have demonstrated that this apparent excess of phosphorus is actually due to the nickel being oxidized. It is now known that, during immersion gold processing, hyperactive corrosion of the nickel-plating occurs on the electroless Ni-P layer.

Tight chemical and process parameter controls need to be in place at printed circuit board manufacturers in order to provide a quality coating of ENIG which meets the IPC-4552 standard. To ensure a problem-free application of ENIG, the correct thickness is recommended in the standard. There should be 0.05 - 0.15 μm of immersion gold applied over 2.50 - 5.00 μm of electroless nickel.

This paper presents results of an investigation of ENIG PWB surface finishes from two manufacturers. The thickness, corrosion behavior and solderability of the finishes were characterized. Further, the quality of the BGA solder joints was evaluated (1) after

* *Corresponding author:*
Dr. Grazyna Koziol
Tele and Radio Research Institute
03-450 Warsaw
Ratuszowa 11, Poland

reflow soldering with Sn / 3.0 Ag / 0.5 Cu paste containing Type 4 of SAC alloy powder and flux type ROL1 (rosin-type, low activity, some halides) or ROL0 (rosin-type, low activity, no halides) and size, and (2) after thermal cycle tests.

Experimental

The thicknesses of the gold and nickel layers were measured by energy dispersive x-ray fluorescence spectrometry. A scanning electron microscope (SEM) with an energy dispersive x-ray (EDX) microanalysis system was used to evaluate the surface morphology at high magnification and identify the elemental chemical composition of a specimen or small area of interest on a sample.

Potentiodynamic polarization and impedance spectroscopy were used to characterize the corrosion behavior in 0.01M NaCl solution in air. Solderability tests were carried out according to IPC/EIA J-STD-003A, Test E: Surface Mount Process Simulation Test.

The components BGA100 (0.8 pitch) and CSP84 (0.5 pitch) were assembled on the boards with ENIG surface finishes from two producers. Lead-free solder paste SAC 305 (Sn / 3.0 Ag / 0.5 Cu), with Type 4 solder powder and ROL0 type flux, was printed on the PCBs by stencil (127 μm thickness) using an MPM Accuflex Speedline automatic printing machine. Components were positioned using a FUJI AIM assembly system and a BTU VIP40 full air convection reflow oven (with five heating zones and one cooling zone) was used to assemble the boards and devices. The peak temperature of the reflow profile and the dwell time above the liquidus temperature (217ºC) were 250ºC and 60 sec, respectively.

Results and discussion

Coating thickness measurement

The thickness of the gold layer on all boards was within the range of 0.07 to 0.15 μm, meeting the requirements of the IPC-4552 standard. The thickness of the nickel layers met the standard requirements except for a few boards in one PWB lot manufactured by Producer A. In this case the measurements showed a differentiation in nickel thickness (from 0.2 to 3.2 μm) across a few single pads on the circuit boards and there were some pads with nickel thicknesses of 2.19 μm. Examples of the thickness measurements are presented in Table 1.

On the pads where the nickel thickness was locally below 1.0 μm, the color of the gold coating was not uniform. In this case some small grey areas were visible. The view of the coating on such pads at high magnifications examined using SEM revealed the different structure of gold layer on grey and golden areas (Fig. 1a). The results of energy dispersive x-ray (EDX) microanalysis are presented in Fig. 1b (element mapping) and Table 2.

The EDX microanalysis indicated a lower concentration of nickel and a higher level of copper on the grey area when compared to the area with the desired gold color. The presence of copper indicates that the thin nickel was ineffective in providing a diffusion barrier against the underlying copper. This undesirable diffusion caused by the thin nickel deposit was directly related to the loosely-attached solder balls.

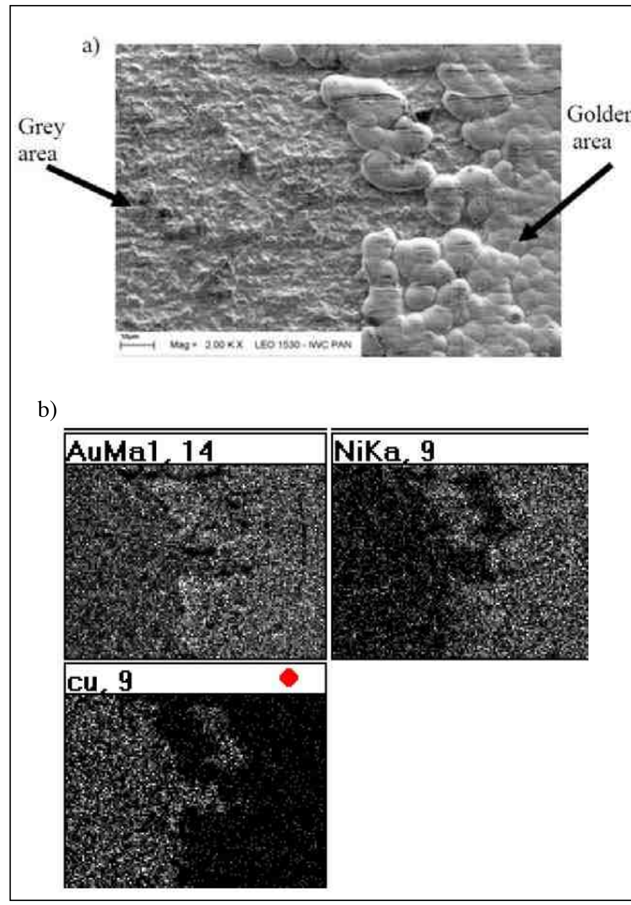

Figure 1—*(a) SEM photograph of an ENIG coating with varying thickness of the nickel layer; (b) EDS mapping of the same area showing changes in gold, nickel and copper concentration (Light areas indicate a thicker layer).*

Table 1

Thickness of nickel and gold layers on the pads of PWBs studied.

Accuracy of the measurements was ± 0.001 µm

	Thickness of layer [μm] and color								
Layer	**Bright area**			**Grey area**			**Uniform color**		
Au	0.084	0.093	0.090	0.069	0.070	0.073	0.052	0.082	0.069
Ni	3.180	3.270	2.960	0.204	0.204	0.520	4.830	2.190	3.380

Solderability

Solderability tests were carried out with two commercially available SAC 305 pastes with Type ROL0 flux and with Type ROL1 flux. The same reflow equipment and process parameters were used as during assembly of the BGA components.

Criteria A (*i.e.*, 99% of each of the surfaces being tested exhibit good wetting, 1% contain only small pin holes and rough spots provided such defects are not concentrated in one area) were obtained for ENIG surfaces with the paste including more active flux (ROL1). For the paste with the less active flux (ROL0), 95% of the tested surfaces exhibited good wetting, and 5% contained dewetted areas and rough spots. No non-wetting or exposed basis metal was observed within the area studied.

The results show that the wettability of the ENIG coatings on all the boards studied from both producers were acceptable for paste with both type of fluxes but better results were obtained for paste with the ROL1 flux.

Solder joint evaluation

All boards were inspected for electrical continuity and for the solder joint quality after reflow soldering with both pastes. The BGA solder joints were examined optically, using the x-ray inspection system and after cross section.

All inspected solder joints passed electrical inspection. X-ray inspection of the solder joints indicated only evidence of voids within the balls. Solder joints with multiple small voids, medium sized voids and large voids were observed on the Producer A ENIG finish with the paste including the less active flux (ROL0), as shown in Fig. 2. Only 2% of the solder joints were free of voids. More than 25% voids in the balls were measured in 16% of the solder joints examined. That means these solder joints did not meet the acceptance criteria of the IPC-A-610D and IPC-7095A standards. Voids were also observed in 95% of the solder joints reflowed with paste including ROL1 flux. However, in this case, the size and area of voids in the balls were smaller. The paste gave small and medium-sized voids that met standards requirements. The percentage of solder joints with voids and the void area percentage data for both pastes were compared and the results are shown in Fig. 3.

Some small voids were observed in the BGA solder joints on the Producer B ENIG samples reflowed with both pastes. The data from the x-ray system with automated BGA voiding calculation showed that fewer voids were noted with the paste including the more active flux (ROL1). Fig. 4 shows cross sectional images of solder joints with voids.

Assembled components were subjected to thermal cycle climatic testing. The climatic test conditions were 85°C at 85% RH. The thermal cycle was a 60 min cycle (-40°C / +125°C) with a 15-min ramp and 15-min dwell.

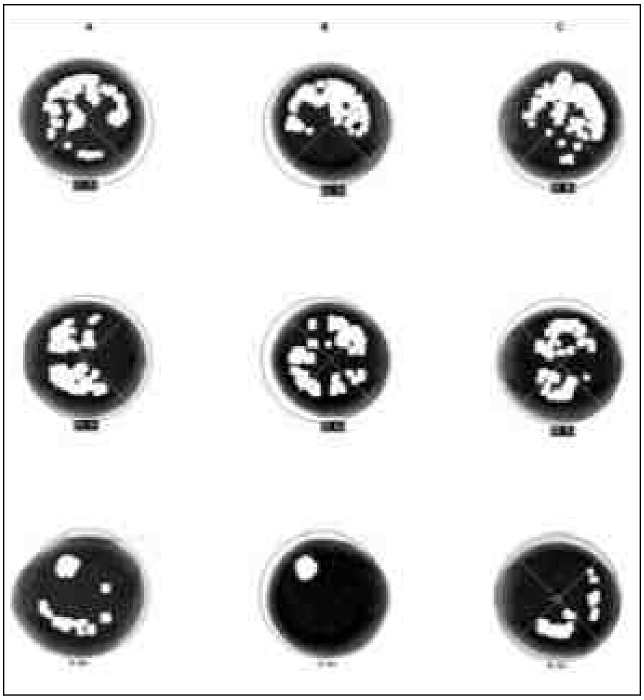

Figure 2—*An example of x-ray images of BGA solder joints with voids (solder paste ROL0 flux, ENIG Producer A).*

Table 2

Results of EDX microanalysis (Mean value from five measurements)

	Intensity Correction	Standard Correction	Element %	Sigma %	Atomic %
Elements	**Gold area of ENIG coating**				
Ni K	1.089	1.00	50.15	1.11	75.15
Cu K	1.048	1.00	2.76	0.76	3.82
Au M	0.712	0.98	47.09	1.10	21.04
	Grey area of ENIG coating				
Ni K	1.093	1.00	11.97	0.78	16.88
Cu K	1.049	1.00	52.25	1.16	68.08
Au M	0.676	0.90	35.78	1.09	15.04

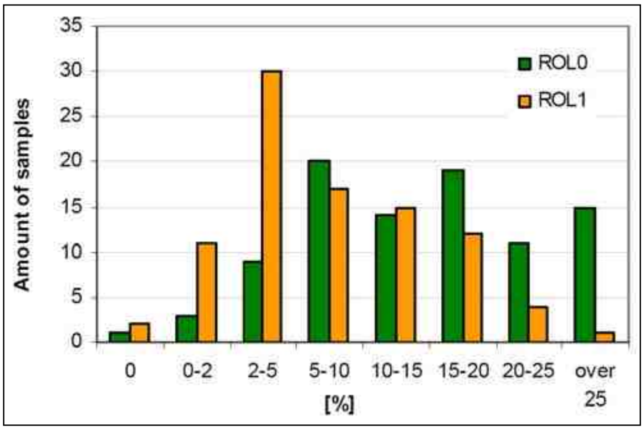

Figure 3—*Comparison of the percentage of solder joints with voids and the void area percentage data for both pastes.*

All boards were inspected for electrical continuity after 500, 1000 and 2000 hr. Cross-sectional micrographs were also produced. Electrical test failures occurred after 2000 hr of thermal cycling and the cross-section revealed interfacial cracks in two BGA balls soldered on the Producer B ENIG and one on the Producer A ENIG, as shown in Fig. 5. The failure criterion was set at 100 Ω for each component daisy-chain. In Fig. 5, propagation of cracks through the void can be seen.

Solder joint defects were also noted for coatings with variable nickel thickness. For these boards, the BGA component was removed after mechanical shocks and examination of the pads showed them to be poorly wetted, as seen in Fig. 6.

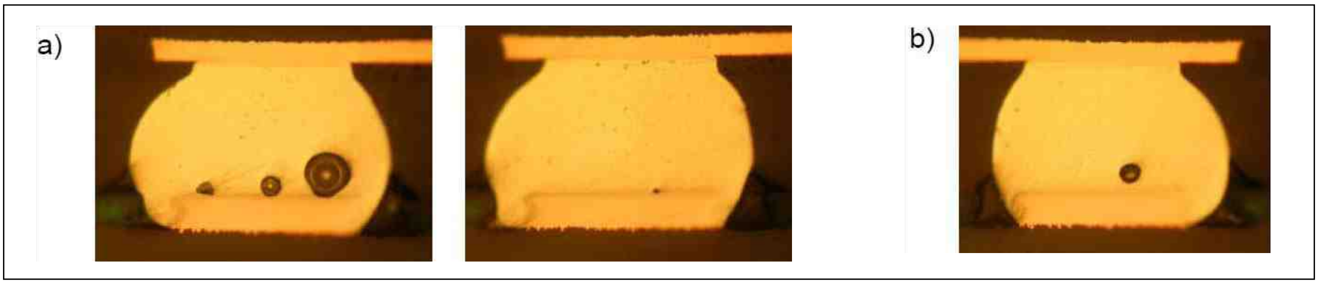

Figure 4—*Examples of BGA solder balls with voids assembled with paste with Type ROL1 flux on ENIG: (a) Producer A; (b) Producer B.*

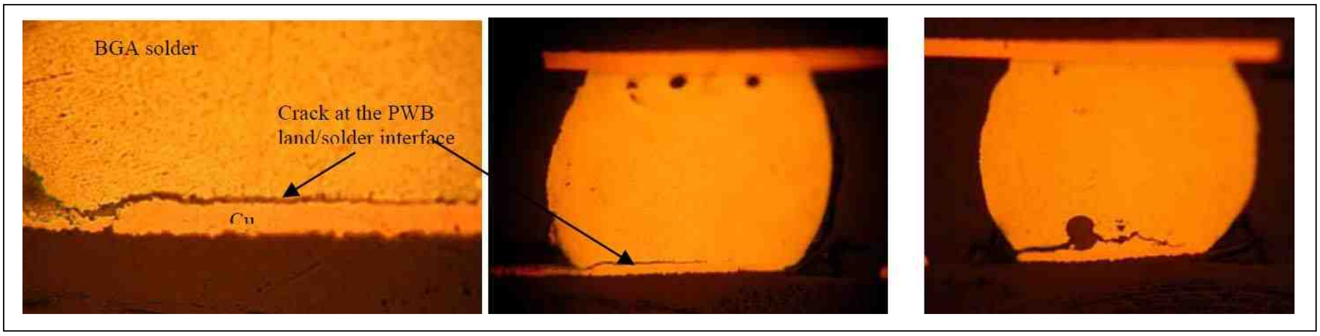

Figure 5—*Cross-sectional micrographs of solder balls with interfacial cracking.*

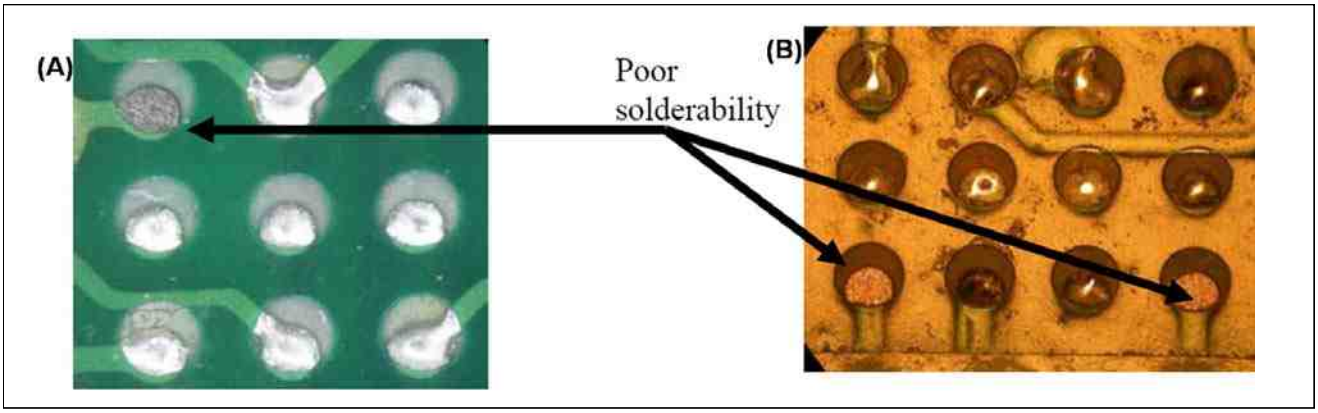

Figure 6—*(a) BGA solder pads after removing BGA component; (b) Examples of poor wettability of pads.*

Intermetallic compounds

EDS analysis of the interfacial structure of the solder joints reveals a layer of $Sn_xCu_yNi_z$ intermetallic compounds, containing medium copper (5 - 29% at%) formed atop the nickel layer. There was also evidence of tin (2 - 4 at%) on the copper layer. Tin is commonly used as an etch resist and should be removed from copper as soon as possible to prevent diffusion of tin into the copper. It is also important to use the proper tin stripping system to remove the tin contamination that would otherwise impede the electroless nickel process, resulting in low nickel.

For some of the solder joints there was a small phosphorus-rich zone detected at the electroless nickel / intermetallic interface. The phosphorus measured was approximately 23.6 at% in these areas, as compared to 12.3 at% in the bulk electroless nickel.

As shown in Fig. 7, EDS analysis of the solder joints with voids identified the presence of silicon, aluminum, nitrogen, bromine and chlorine. The elemental levels were determined by EDS standardless quantitative analysis. The results of the measurements show much higher concentrations of Al, Si, Br and Cl in the voids area when compared to the respective concentrations in the layers of nickel and intermetallic, as well as the bulk of the solder ball. In the IMC layer and bulk of the solder, the aluminum content was approximately 2 at%, silicon 5 At% and bromine 2 at%. In the void area, the results were as high as 60, 28 and 24 at% for aluminum, silicon and bromine, respectively (Table 3).

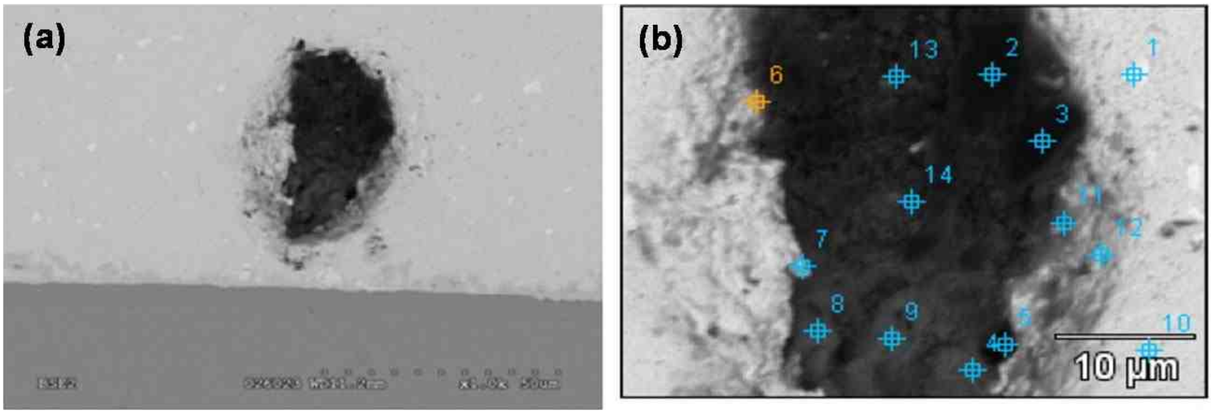

Figure 7—*SEM images of (a) solder joints with voids and (b) the voids area with points of composition measurements given in Table 3.*

Table 3

Results of EDS measurements in the selected points of the void area shown in Fig. 7

No.	Atomic %								
	Ni	Cu	Sn	Au	Br	N	Al	Si	Cl
1	0.85	0.83	34.78	6.22	-	57.33	-	-	-
2	-	21.11	87.89	-	-	-	-	-	-
3	-	28.94	47.12	-	23.94	-	-	-	-
4	-	3.7	36.79	-	-	-	52.21	-	-
5	-	5.25	89.94	-	-	-	4.91	-	-
6	-	9.34	46.30	-	-	-	26.91	15.69	1.76
7	-	1.09	36.35	-	-	49.27	7.66	5.20	0.42
8	-	5.53	45.25	-	-	-	38.14	11.08	-
9	-	5.53	45.25	-	-	-	38.14	11.08	-
10	-	2.13	42.99	-	-	50.37	4.5		
11	8.68	11.39	40.57	-	-	-	34.68	4.67	-
12	6.75	11.63	25.99	-	-	50.22	5.42	-	-
13	-	14.26	10.47	-	-	-	60.51	9.96	4.8
14	-	6.20	10.85	-	-	-	53.44	28.39	1.11

The electroless nickel process chemistry involves very high temperatures and is very aggressive. However, by the time the contamination is broken down, the nickel may plate below the required thickness where the contaminants covered the copper.

Corrosion resistance

The corrosion properties of ENIG coatings were determined on the basis of potentiodynamic polarization experiments in 0.01M NaCl solution in air. The scanning rate during potentiodynamic polarization was 5 mV/sec and potential applied to the test electrode ranged from -500 mV to +500 mV versus the rest potential. An Autolab set with GPES 4.4 and FRA 2.3 software was used.[6] The investigation was made in a three-electrode cell with a platinum counter electrode. The working electrode was the test sample with surface area of 1.1 cm^2 and saturated calomel electrode (SCE) was used as the reference electrode. The measurements were done after 0.5 hr of exposure to the solution. The results of potentiodynamic polarization measurements for the ENIG layer with different nickel underlayer thicknesses are presented in Fig. 8 and Table 4.

There are visible differences between the curves obtained for layers with different nickel thicknesses. The lowest values of anodic and cathodic corrosion current density (I_{corr}) were recorded for Sample 2 with a thicker layer of nickel and highest for Sample 3 (the thinner nickel thickness). This means that the corrosion rate is the highest for gold on Sample 3 and the lowest on Sample 2. The existence of locally thinner nickel areas on pads increases the corrosion rate, but because of their small area, their influence on the corrosion rate was lower than for Sample 3.

The values of corrosion current density (I_{corr}), charge transfer resistance (R_{ct}) and polarization resistance (R_p) were calculated from analysis of the polarization curves and compiled in Table 4. This data shows that immersion gold on thinner nickel layers exhibits higher corrosion rates.

The resistance values increased in the sequence: Sample 3 < Sample 1 < Sample 2. The relation for current density is the opposite. Both parameters indicate that the greatest resistance to corrosion is obtained with an ENIG coating with a 3.74-μm thick nickel underlayer. The lowest resistance was found for an ENIG coating with a nickel thickness of 2.19 μm.

Results for the corrosion behavior of gold indicated that a decrease in nickel thickness leads to reduced corrosion resistance. The decrease in the corrosion current density and an increase in the polarization / charge transfer were also observed in the case of an ENIG deposit with an average nickel thickness of 3.74 μm and at least 0.52 μm locally.

Conclusions

The thickness, corrosion behavior and solderability of ENIG PWB surface finishes from two manufacturers and the influence of these finishes on BGA solder joint quality were investigated.

The results indicate that the thickness and uniformity of the nickel layer affects intermetallic formation and the mechanical strength of Sn-Ag-Cu solder joints. Some problems with non-wetting pads were noted on pads with nickel thicknesses below 2.5 μm and with differentiation in nickel thickness from 0.2 to 3.2 μm across a pad.

Observation of the corrosion behavior of gold indicated that decrease in nickel thickness leads to decreased corrosion resistance. Further, even a small local deviation in the thickness of the nickel underlayer on a single solder pad of a PWB contributes to a decrease in corrosion resistance of the ENIG finish.

Other surface defects were found, including evidence of tin (2 - 4 At%) on the top of copper layer, a small phosphorus-rich zone on the interface of the Ni/P -IMC layer and the presence of silicon, aluminum, nitrogen, bromine and chlorine. All were found to be closely related to the quality of maintenance and operation of the ENIG plating process at the circuit board manufacturers.

Table 4

Corrosion parameters for layers with different nickel underlayer thicknesses (an average value of five measurements)

Sample No.	E_{corr}, V_{NEK}	R_p, kOhm•cm²	I_{corr}, μA/cm²
1	-0.192	1.7	0.19
2	-0.299	5.8	0.011
3	-0.211	0.2	0.50

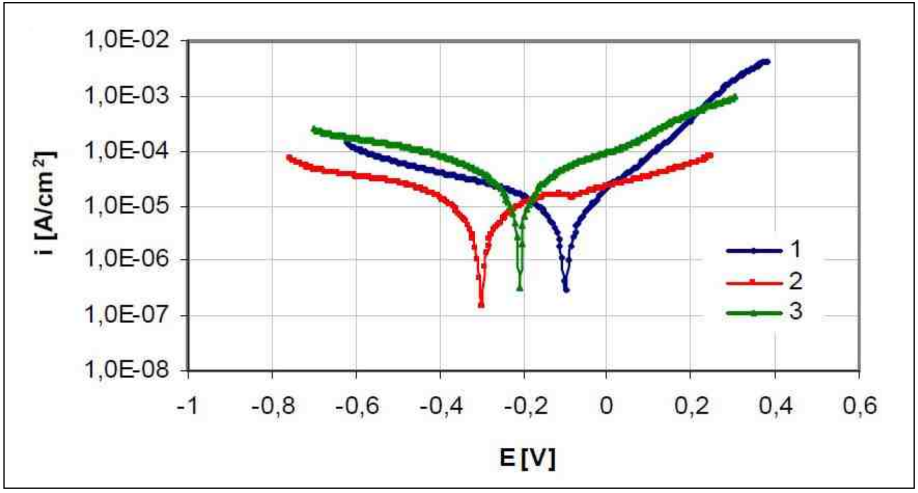

Figure 8—*Polarization curves for layers with different nickel underlayer thicknesses. An average nickel thickness on samples studied was, respectively: #1: 3.74 µm on the light area and 0.52 µm on the grey area: #2: 4.83 µm; #3: 2.19 µm.*

Acceptable solderability of the pads was obtained by using a solder paste which included a more active flux. Nonetheless, some solder defects were still produced under conditions of thermal cycling or mechanical shock.

Acknowledgement

The Polish State Committee for Scientific Research supported these works, Project No. R02 041 02.

References

1. K. Bukat & H. Hackiewicz, *Lutowanie bezołowiowe (Lead-free Soldering)*, BTC, Warszawa, Poland, 2007.
2. K. Pun, P. Eu, M.N. Islam, C.Q. Cui, "Effect of Ni Layer Thickness on Intermetallic Formation and Mechanical Strength of Sn-Ag-Cu Solder Joint", *Proc. 10th Electronic Packaging Technology Conference, EPTC 2008*, IEEE, New York, NY; p. 487.
3. C.W. Nielsen, *et al.*, "New Trends for PWB Surface Finishes in Mobile Phone Applications," *Proc. Pan Pacific Microelectronics Symposium 2006,* Surface Mount Technology Association (SMTA), Edina, MN, 2006.
4. A. Sargent, J. Konrad & J. Collura, "Corrosion Resistance of ENIG: An Improved Immersion Gold Process," *Circuitree*, **16** (12), 10 (2003); http://www.circuitree.com/Articles/Feature_Article/0616a7f2010f7010VgnVCM100000f932a8c0____ .
5. Z. Mei, M. Kaufmann and P. Johnson, "Interfacial Fracture of BGA Packages on Electroless Ni/ Immersion Au and its Relation to Plating Process," *IPC National Conference Proceedings: A summit on PWB Surface Finishes and Solderability, September 1997*, IPC, Bannockburn, IL, (1997); pp. 23-45.
6. *Autolab User Manual, Electrochemical Instruments*, Eco-chemie BV, Utrecht, The Netherlands, 1995.

About the authors

Dr. Grazyna Koziol is the Head of the Printed Circuit Research Department of Tele- and Radio Research Institute (ITR). She is also the Coordinator of the Centre for Advanced Technology of Electronic Interconnections at ITR. She obtained her Doctor of Science degree from the Chemical Department of Warsaw Technology University in 2000.

Aneta Arazna is a Research Assistant at the Printed Circuit Research Department of Tele- and Radio Research Institute (ITR). She received her M.Sc.Eng. degree from the Department of Technological Chemistry of Warsaw University of Technology (PW) in 2002. She is currently working in ITR and is also a Doctoral student at Warsaw University of Technology.

Wojciech Steplewski is a Research Assistant at the Printed Circuit Research Department of Tele- and Radio Research Institute (ITR). He received his M.Sc.Eng. degree in Materials Engineering from the Mechanical Department of Cracov University of Technology in 2000.